Journal of Organometallic Chemistry, 470 (1994) 147–152

Nuclear magnetic resonance studies of sulfur inversion in bis(cyclopentadienyl)-molybdenum and -tungsten complexes with dithioethers

José R. Ascenso [a], Maria de Deus Carvalho [b], Alberto R. Dias [a], Carlos C. Romão [c], Maria J. Calhorda [c] and Luis F. Veiros [a]

[a] *Centro de Química Estrutural, Instituto Superior Técnico, 1096 Lisboa Codex (Portugal)*
[b] *Departamento de Química, Faculdade de Ciências de Lisboa, R. Ernesto de Vasconcelos, Edifício C1, 1700 Lisboa (Portugal)*
[c] *Instituto de Tecnologia Química e Biológica, Rua da Quinta Grande 6, 2780 Oeiras (Portugal) and Instituto Superior Técnico, Av. Rovisco Pais, 1096 Lisboa Codex (Portugal)*

(Received July 28, 1993)

Abstract

The metallocene thioether derivatives $[Cp_2M(MeSCH_2CH_2SMe)][PF_6]_2$ (**1**, M = Mo; **2**, M = W), $[Cp_2Mo(SCH_2CH_2SMe)][PF_6]$ (**3**) and $[Cp_2M(SCH_2CH_2S)]$ (**4**, M = Mo; **5**, M = W) exhibit temperature-dependent fluxional behavior in solution, owing to the pyramidal sulfur inversion process. The activation energies for this process were determined from proton band-shape analysis in the cases of **1** (54.9 ± 2 kJ mol^{-1}), **2** (51.2 ± 4.6 kJ mol^{-1}) and **3** (30.0 ± 3.1 kJ mol^{-1}). Extended Hückel calculations on related model complexes suggest that local inversion at the sulfur atoms, rather that an inversion of the complete S–C–C–S chain, is responsible for the observed fluxional behaviour.

Key words: Tungsten; Molybdenum; Nuclear magnetic resonance; Dithioether; Sulfur inversion; Extended Hückel calculations

1. Introduction

Sulfur inversion has been extensively studied by Abel and co-workers using NMR techniques in a wide variety of transition metal complexes [1]. However, in bis(cyclopentadienyl) transition metal complexes such processes are not so well documented. The temperature-dependence of the ^{1}H NMR spectra of a series of bis(cyclopentadienyl) dimetal thiolate bridged complexes, $[Cp_2Ti(\mu\text{-}SMe)_2MCl_2]$ (M = Pd or Pt), $[Cp_2Ti(\mu\text{-}SR)_2M(CO)_4]$ (R = H or Me; M = Mo or W), $[Cp_2Ti(\mu\text{-}SR)_2NiCp][BF_4]$ (R = Me or Ph) and $[Cp_2Ti(\mu\text{-}SEt)_2CuL][PF_6]$ (L = phosphine or pyridine) has been correlated with a *cis–trans* isomerization equilibrium that probably involves a pyramidal inversion at sulfur [2], but no further investigation has, to our knowledge, appeared in the literature concerning the mechanism of isomerization in this class of complexes.

In order to assess the importance of the steric and electronic effects of the Cp_2M moiety on sulfur inversion barriers, we have prepared a series of simple metallocene dithioether derivatives $[Cp_2M(MeSCH_2CH_2SMe)][PF_6]_2$ (**1**, M = Mo; **2**, M = W), $[Cp_2Mo(SCH_2CH_2SMe)][PF_6]$ (**3**), $[Cp_2M(SCH_2CH_2S)]$ (**4**, M = Mo; **5**, M = W) and a detailed study of the proton line shape-dependence on temperature was undertaken. Extended Hückel calculations [3] on suitable model complexes provide further insight into the nature of the mechanism responsible for spectral changes.

2. Results and discussion

2.1. Preparation of $[Cp_2M(dth)][PF_6]_2$

The general route to cationic derivatives of molybdenocene and tungstenocene, $[Cp_2ML_2]^{2+}$ involves

Correspondence to: Professor J.R. Ascenso.

0022-328X/94/$7.00
SSDI 0022-328X(93)24186-9

substitution of the parent dihalides, normally assisted by halide abstraction with $Tl[PF_6]$ or $Tl[BF_4]$ [4].

However, to prepare complexes of thioethers an alternative approach is necessary, because of their weak nucleophilicity. This is depicted in eqn. (1), which takes advantage of the high nucleophilicity of the coordinated S atoms of the thiolate in $[Cp_2M(SCH_2CH_2S)]$.

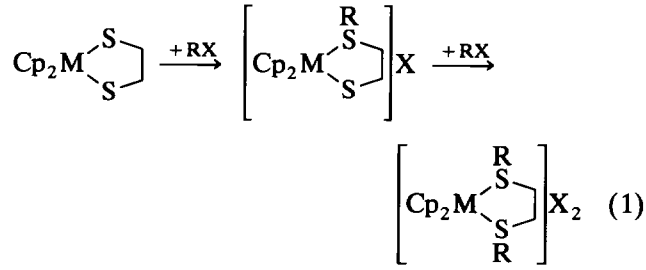

(1)

This method was first used in Group 6 metallocene thiolate chemistry by Green and co-workers [5] in the preparation of the first thioether derivatives of these metallocenes. In this way, the cations $[Cp_2Mo(SCH_2CH_2SMe)]^+$ (**3**) [4] and $[Cp_2W(SCH_2CH_2SR)]^+$ (R = Me, CH_2Ph, C_3H_5) [6] were obtained from $[Cp_2M(SCH_2CH_2S)]$ (M = Mo or W). Large excess of MeI and longer reaction times favour the second alkylation. The resulting new dications $[Cp_2M(dth)][PF_6]_2$ (**1**, M = Mo; **2**, M = W; dth = $MeSCH_2CH_2SMe$) are readily isolated as $[PF_6]^-$ salts, as described in the Experimental section. These orange, air-stable complexes behave as 2:1 electrolytes in $MeNO_2$ and were fully characterized by analytical and spectroscopic methods.

2.2. NMR studies

The coordination around the metal in the cationic complexes **1**, **2** and **3**, as well as in their non-alkylated neutral precursors $[Cp_2M(SCH_2CH_2S)]$ (**4**, M = Mo; **5**, M = W) is pseudotetrahedral and each alkylated sulfur atom of the dithioether is chiral. Diasteriomers may then exist, leading to NMR-distinguishable *syn* and *anti* forms. As shown in Scheme 1, inversion at a single sulfur site interconverts the *syn* and *anti* forms, whereas the *syn–syn* and *anti–anti* interconversions need a simultaneous inversion at both S atoms.

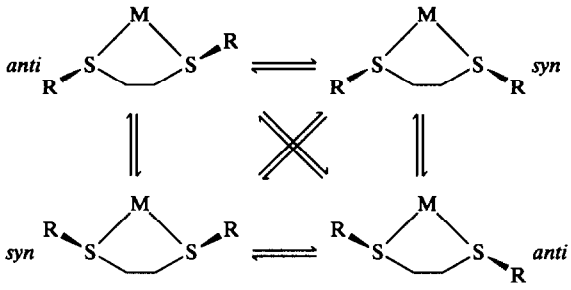

Scheme 1.

TABLE 1. Proton chemical shifts (ppm) of compounds **1–5** in the slow and fast exchange limits

	T (°C)	C_5H_5	SCH_2CH_2S	CH_3
1	30	6.24	3.29	2.90
	−80	6.35	4.07; 2.62	2.96
2	30	6.24	3.03	3.10
	−80	6.33	3.64; 2.49	3.14
3	30	5.59	2.89; 2.30	2.69
	−80	5.73; 5.61	3.28; 2.45	2.73
4	30	5.10	2.26	–
5	30	5.05	1.83	–

The effect of sulfur inversion on the ^1H NMR spectra of complexes **1** to **5** was monitored from room temperature down to −80°C and the ^1H chemical shifts are shown in Table 1 at both limits.

At room temperature, sulfur inversion is sufficiently fast to render two Cp groups in all the compounds and the methylene protons of the dithioether in **1** and **2** equivalent. In the same way, the two Me substituent groups at sulfur in compounds **1** and **2** also become equivalent. A limiting static spectrum is obtained for compounds **1**, **2** and **3** at −80°C.

In compounds **1** and **2** the methylene protons give rise to a widely spaced AA'BB' multiplet that in the case of **2** looks very like an AB quartet. The resonances of the Cp and S–Me protons always remain sharp singlets over this range of temperature. Accordingly, the *anti* isomers are the only existing ones observed, as the *syn* isomers would lead to the nonequivalence of the two Cp groups in the limiting low temperature spectrum.

The preference of the metallacycles **1** and **2** for *anti* isomers in solution is in marked contrast with previous results for octahedral dithioether complexes of Pt [7], Mo, and W [8,9], where an equilibrium between *syn* and *anti* forms was observed in solution. Molecular models suggest that the preference of these metallacycles for an *anti* configuration may be because accommodation of two methyl groups near the Cp ring in the *syn* form (as opposed to only one Me near the Cp ring in the *anti*) would require more distortion of the complex frame to avoid strong repulsive interactions.

In the case of compound **3**, the rates of inversion for the two sulfur atoms are very different. The unsubstituted S atom is always inverting very fast on the NMR time scale, whereas the S–Me group inverts much more slowly, leading to exchange-broadened proton resonances for the Cp and methylenic protons. The limiting spectrum at −80°C comprises two singlets of equal intensity for the Cp protons and a complex pattern for the methylene protons of the dithioether ligand.

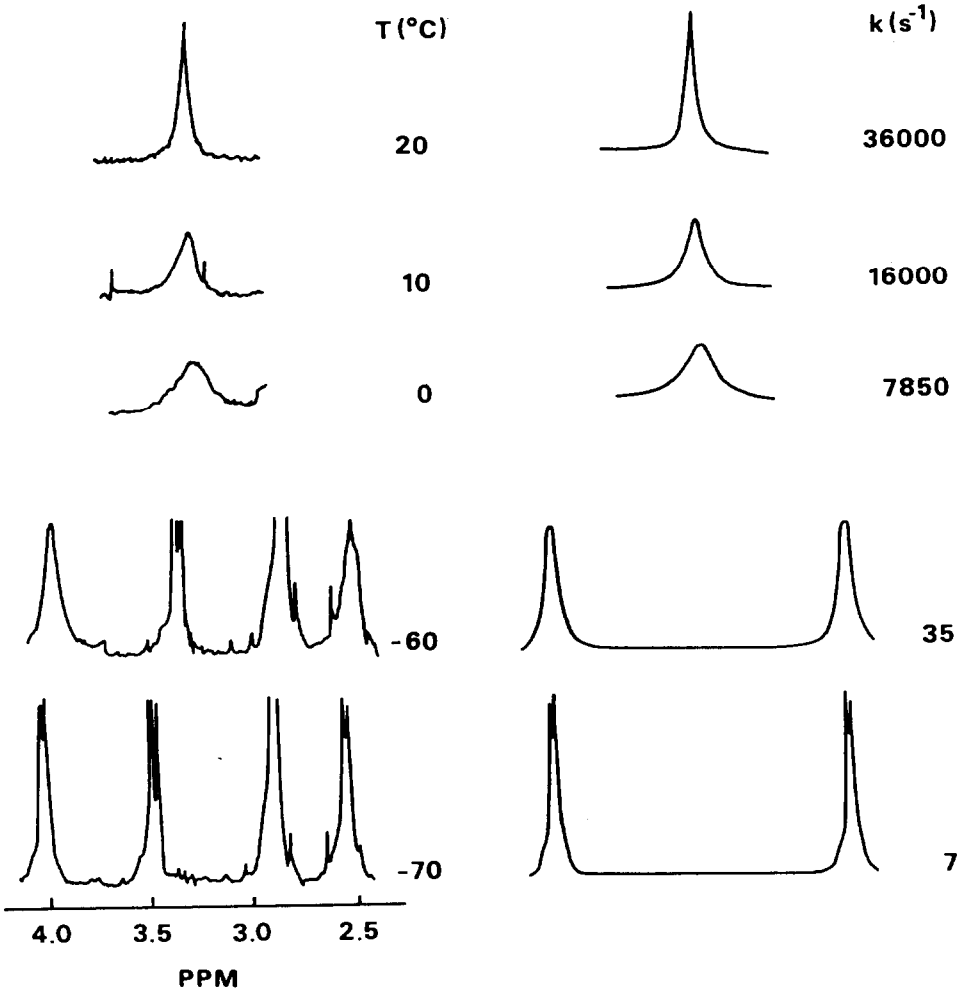

Fig. 1. Experimental (left) and simulated (right) proton spectra of the methylene region of *cis*-$[Cp_2Mo(dth)][PF_6]_2$ in the temperature range −70°C to 20°C.

In the remaining metallacycles **4** and **5**, both S atoms invert extremely rapidly in the NMR time scale and no effect of the temperature on the ^1H NMR spectrum was observed down to −80°C.

The two *anti* isomers of compounds **1** and **2** shown in Scheme 1 are not distinguishable by ^1H NMR spectroscopy, because both lead to an average AA'BB' multiplet for the methylene protons of the dithioether. Interconversion of the *anti* isomers by a two-site sulfur inversion interchanges the A and B methylene proton environments and leads to the collapse of the low-temperature AA'BB' multiplet to a singlet at room temperature. In order to determine the rate constants of the process of sulfur inversion, the resulting exchange broadened proton methylenic spectra were simulated on the basis of a AA'BB' ⇔ BB'AA' spin exchange mechanism over the range of temperatures from 20 to −70°C, as described in the Experimental section. The result of these simulations for compound **1** is shown in Fig. 1.

The static proton parameters used in these simulations are given in Table 2. Coupling constants were determined by spin simulation of the limiting average AA'BB' methylene multiplet at −80°C for **1** and **2**.

TABLE 2. Static parameters used for simulation of the methylene proton spectra of complexes **1** and **2** and for the Cp protons spectra of **3**

	T_2^* (s)	ν_A(Hz)	ν_B(Hz)	J(AA)'	J(AB) = J(A'B')	J(AB') = J(A'B)	J(BB')
1	0.066	782.23	1207.89	11.8	−11.9	4.1	1.9
2	0.090	741.99	1083.79	3.0	−8.9	1.8	1.5
3	0.21	1703.11	1677.72	–	–	–	–

At −80°C.

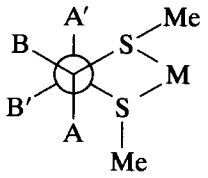

Scheme 2.

The spin simulation of the multiplet of **2** was found to be particularly difficult, owing to the small number of lines in the AA'BB' multiplet of this compound.

The rates of sulfur inversion for compound **3** were determined by simulation of the exchange-broadened resonance of the Cp protons at several temperatures. A simple A ⇔ B spin exchange process between two uncoupled sites was taken as basis for the simulations. The static parameters used on these simulations were determined from the ^{1}H spectrum at −80°C and are also given in Table 3.

The two sets of average coupling constants for **1** and **2** given in Table 2 show substantial differences. For compound **1** the values of the vicinal coupling constants J(AA'), J(BB') and J(A'B) = J(AB') are consistent with a twisted conformation of the metallacycle ring with the hydrogen atoms in a staggered arrangement (Scheme 2).

A similar metallacycle ring conformation was deduced from methylene proton-proton coupling constants of the ligand 2,7-dimethyl-3,5-diselenaoctane in a series of complexes with Pd, Cr, Mo, and W [10]. The set of coupling constants for compound **2** suggests a similar but less-twisted conformation for the metallacycle ring.

The chemical shifts of the lines in the AA'BB' multiplet of compound **1** are independent of temperature. However, for complex **2** the chemical shifts of the corresponding lines show a small dependence of 0.07 Hz per °C and it was necessary to use this drift to correct their positions in the intermediate- and fast-exchange regions. The other static parameters, including those for compound **3** in Table 2, were found to be constant with temperature in the slow-exchange region, and were assumed to remain constant through the intermediate- and fast-exchange regions.

The Arrhenius and Eyring activation parameters for sulfur inversion in metallacycles **1**, **2** and **3** are given in Table 3. The magnitudes of the activation energies E_a and $\Delta G^{\ddagger}$ are about the same in compounds **1** and **2**, and are rather lower than found for sulfur-inversion processes in *cis*-[M(CO)$_4$(dth)] (M = Mo or W) complexes [8,9]. This is probably a consequence of the steric constraints imposed by the two bulky Cp rings, that would stabilize the planar transition state of sulfur through an increase in bond angles around these atoms.

The activation energy obtained for compound **3**, E_a = 30.0 kJ mol^{-1}, is about half of the value found in compounds **1** and **2**, reflecting a much more hindered sulfur inversion at methyl-S compared to that at the thiolato-S atom. This difference in the values of E_a was not paralleled by the $\Delta G^{\ddagger}$ values, since a high negative entropy value ($\Delta S^{\ddagger}$ = −86.6 J K^{-1} mol^{-1}), was found for compound **3** in deuterated methanol. Whether this corresponds to increased order in the solvent cage of the activated complex or to another type of solvent assistance (including coordination) on the process of sulfur inversion, cannot be inferred from the present data.

2.3. Molecular orbital calculations

Extended Hückel molecular orbital calculations were therefore made in order to understand the nature of the inversion mechanism. As sketched in Scheme 1, two different processes may occur: separate inversions at each sulfur atom or an inversion of the complete metallacycle. While it is easy to deduce that the absence of sulfur substituents greatly facilitates any of these possibilities, leading to the very fast exchanges observed for the neutral, non-alkylated complexes **4** and **5**, and also for half of **3**, NMR data by themselves are not sufficient to define the mechanism.

The two complexes used as models in the calculations were tungsten analogues of **1** and **2** [Cp$_2$W(RS-CH$_2$CH$_2$SR]$^{2+}$, R = H or CH$_3$. Their geometry had to be optimized as no acceptable X-ray structure determination could be obtained. By geometry optimization, we mean here essentially finding the conformation of the SCCS chain, either zig-zag chain or planar (Scheme 3), as the rest of the molecule can be accurately modelled from the many structures known for biscyclopentadienyl derivatives [12].

TABLE 3. Activation parameters for pyramidal inversion at sulfur in complexes **1**, **2** and **3**

	E_a (kJ mol^{-1})	log A	$\Delta H^{\ddagger}$ (kJ mol^{-1})	$\Delta S^{\ddagger}$ (J K^{-1} mol^{-1})	$\Delta G^{\ddagger}_{298}$ (kJ mol^{-1})
1	54.9 ± 2.0	14.3 ± 0.2	52.9 ± 1.6	21.2 ± 1.4	46.5 ± 0.7
2	51.2 ± 4.6	13.7 ± 0.3	49.2 ± 4.6	10.2 ± 6.1	46.6 ± 2.8
3	30.0 ± 3.1	8.6 ± 0.2	27.9 ± 3.1	−86.6 ± 2.3	53.7 ± 2.4

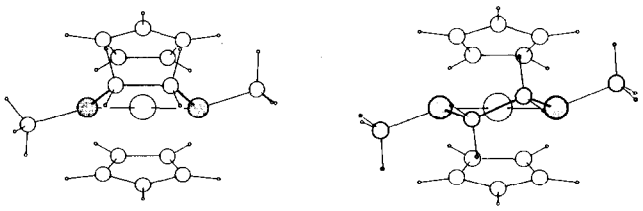

Scheme 3.

TABLE 4. Calculated activation energies for the sulfur-inversion mechanisms

Complex	S inversion (kJ mol^{-1})	Chain inversion (kJ mol^{-1})
$[Cp_2W(CH_3SCH_2CH_2SCH_3)]^{2+}$	25.9	168.9
$[Cp_2W(HSCH_2CH_2SH)]^{2+}$	25.8	167.6

Our results show close energy values for those two extreme structures, in good agreement with the NMR experimental data for complex **2** (previous section). Hence, all the calculations were performed on the two structures producing qualitatively similar results, although the zig-zag conformation was 12 kJ mol^{-1} more stable than the planar for both models. For simplicity we present only the results obtained with this conformation.

Having determined the most probable structure for the complexes, we then probed the two inversion mechanisms mentioned above. This was done for the two models by estimating as activation energy the energy differences between the initial and the transition state structures for both mechanisms. Thus, in the case of an inversion of the complete metallacycle, the transition state corresponds to a complex having a totally planar ring (Scheme 4). On the other hand, two simultaneous inversions localized at the sulfur atoms lead to a transition state structure with a planar environment around these atoms, and result in a sp^2-like geometry around each sulfur atom (Scheme 4). The results are shown in Table 4.

Calculations were also done for related molecules with non-alkylated sulfur atoms, which showed, as expected, smaller barriers for inversion. However, the study of $[W(CO)_4(dth)]$ revealed higher activation energies for both mechanisms, reflecting an equilibrium geometry more different from the transition state. In the absence of close Cp rings, the sulfur atoms adopt a more pyramidalized geometry.

A comparison of the results with the experimental NMR data (Table 3) suggests the localized inversion mechanism to be the more likely one. Indeed, the activation energy associated with an inversion of the whole metallacycle is about one order of magnitude greater than both the experimental data and the results of the calculations for the competing mechanism.

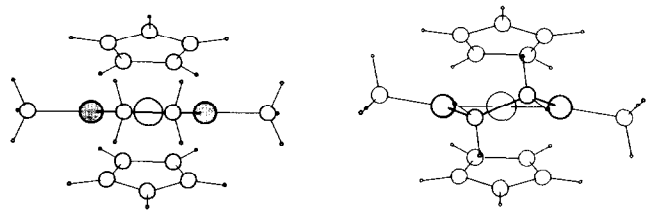

Scheme 4.

Although the calculated energies for the localized sulfur inversions are of the same order of magnitude as the experimental ones, they are still about 50% smaller. This is not surprising considering the qualitative nature of the method used and the simplified choice of the two transition states, not to mention the unaccountable factors which play a role in experiments where molecules are not isolated. In spite of these limitations, NMR data and theoretical calculations indicate strongly a localized inversion at each sulfur atom.

3. Experimental details

The complexes were prepared using standard Schlenk techniques under argon $[Cp_2M(SCH_2CH_2S)]$ (M = Mo or W) [6] and $[Cp_2Mo(SCH_2CH_2SMe)]^+$ (**3**) [4] were prepared according to literature methods. Acetone and dichloromethane were dried over 4A molecular sieves.

3.1. Preparation of $[Cp_2Mo(dth)][PF_6]_2$

$[Cp_2Mo(SCH_2CH_2S)]$ (0.218 g; 0.68 mmol) was suspended in dry acetone (15 ml) and treated with an excess of MeI (4.5 ml). The mixture was vigorously stirred for 12 h and the brick-red precipitate was then filtered off and washed with acetone. Dissolution of this precipitate in the minimum amount of water and addition of a saturated solution of $[NH_4][PF_6]$ gave an abundant orange precipitate which was filtered off and thoroughly washed with water. The product was recrystallized from acetone/ethanol by slow evaporation, filtered, washed with ethanol and dried under vacuum. Yield: 80%. Anal. Found: C, 26.2; H, 3.3. $C_{14}H_{20}F_{12}MoP_2S_2$ calc.: C, 26.3; H, 3.2% $\Lambda_M = 218\ \Omega^{-1}\ cm^2\ mol^{-1}$ (10^{-3} M in NO_2Me).

3.2. Preparation of $[Cp_2W(dth)][PF_6]_2$

$[Cp_2W(SCH_2CH_2S)]$ (0.7 g; 1.75 mmol) was dissolved in CH_2Cl_2 (50 ml) and treated with an excess of MeI (4 ml). The mixture was heated under reflux for 2 h and stirred at room temperature for a further 12 h. The precipitate was collected by filtration and worked-

up and recrystallized as described above, to give orange crystals. Yield 85%. Anal. Found: C, 23.6; H, 2.8. $C_{14}H_{20}F_{12}P_2S_2W$ calc.: C, 23.2; H, 2.8% $\Lambda_M = 203$ Ω^{-1} cm^2 mol^{-1} (10^{-3} M in NO_2Me).

3.3. NMR measurements

^{1}H NMR spectra of complexes **1–5** were run on a CXP 300 Bruker spectrometer equipped with a standard variable-temperature unit. This unit was previously calibrated by inserting a copper-constantan thermocouple into the NMR probe. To obtain better precision in temperature measurements, the extremity of the thermocouple was fixed inside a 5-mm NMR tube at the height of the receiver coil. Temperature readouts are considered accurate to ± 1°C.

Line-shape simulations of the variable-temperature 1H NMR spectra were performed using a modified version of the DNMR5 program of Kleier and Binsh [11]. The quality of each simulated spectrum was assesssed by visual comparison with the experimental spectrum.

Simulations of the limiting AA'BB' methylene proton multiplet in **1** and **2** at -80°C were obtained by using the spin-simulation program PANIC (Bruker).

Typical proton spectra of complexes were run in deuterated acetone (**1** and **2**), deuterated methanol (**3**), and deuterated dichloromethane (**4** and **5**). In all cases, tetramethylsilane was used as internal reference.

3.4. Molecular orbital calculations

All the calculations were of the extended Hückel type [3] with modified H_{ij}'s [13]. The basis set for tungsten consisted of 6s, 6p and 5d orbitals. Only s and p orbitals were used for sulfur. The s and p orbitals were described by single Slater-type wave functions, and d orbitals were taken as contracted linear combinations of two Slater-type wave functions.

Standard parameters were used for S, C and H [3], while those used for tungsten were as follows: 6s, $H_{ii} = -8.26$ eV, $\zeta = 2.341$; 6p, $H_{ii} = -5.17$ eV, $\zeta = 2.309$; 5d, $H_{ii} = -10.37$ eV, $\zeta_1 = 4.982$, $\zeta_2 = 2.068$, $C_1 = 0.6940$, $C_2 = 0.5631$.

The distances (pm) and angles (deg) used to build the models were as follows: W–Cp = 200, W–S = 249, S–C = 178, S–C (Me) = 176, C–C = 156, C–C (Cp) = 140, C–H = 108, S–H = 134; Cp–W–Cp = 132, S–W–S = 79. The S–C–C–S dihedral and bond angles of the chain substituents were optimized by energy minimization for each structure.

References

1 E.W. Abel, S.K. Bhargava and K.G. Orrell, *Prog. Inorg. Chem., 32* (1984) 1.

2 (a) G. Wilkinson, F.G.A. Stone and E.W. Abel (eds.), *Comprehensive Organometallic Chemistry*; Pergamon Press, Oxford, 1982; (b) D.W. Stephan, *Coord. Chem. Rev., 95* (1989) 41.

3 (a) R. Hoffmann, *J. Chem. Phys., 39* (1963) 1397; (b) R. Hoffmann and W.N. Lipscomb, *J. Chem. Phys., 36* (1962) 2179.

4 A.R. Dias and C.C. Romão, *J. Organomet. Chem., 233* (1982) 223.

5 M.L.H. Green and W.E. Lindsell, *J. Chem. Soc. (A)*, (1967) 1455.

6 M.G. Harriss, M.L.H. Green and W.E. Lindsell, *J. Chem. Soc. (A)*, (1969) 1453.

7 K.G. Orrell, *Coord. Chem. Rev., 96* (1989) 1.

8 E.W. Abel, I. Moss, K.G. Orrell and V. Sik, *J. Organomet. Chem., 326* (1987) 187.

9 E.W. Abel, D.E. Budgen, I. Moss, K.G. Orrell and V. Sik, *J. Organomet. Chem., 362* (1989) 105.

10 G. Hunter and R.C. Massey, *J. Chem. Soc., Dalton Trans.*, (1976) 2007.

11 D.S. Stephenson and G. Binsh, DNMR5 Program, Institute of Organic Chemistry, University of Munich, 1978.

12 M.J. Calhorda and A.M. Galvão, in M. Gielen (ed.), *Topics in Physical Organometallic Chemistry*, pp. 93–138, Freund Publishing House, Tel-Aviv, 1992.

13 J.H. Ammeter, H.-B. Bürgi, J.C. Thibeault and R. Hoffmann, *J. Am. Chem. Soc.*, (1978) 100, 3686.